Original Paper

Numerical analysis of cooling potential and indoor thermal comfort with a novel hybrid radiant cooling system in hot and humid climates

Jiying Liu[1] (ID)**, Moon Keun Kim[2]** (ID) **and Jelena Srebric[3]**

Abstract

The study investigates a hybrid radiant cooling system's potential to achieve thermal comfort. The hybrid radiant cooling (HRC) system combines the best features of a typical all-air and conventional chilled radiant cooling system. An HRC system presents the advantages to (a) reduce vapour condensation and to (b) adjust the cooling output by using an Airbox convector. The three systems perceive thermal comfort in the predicted mean vote (PMV) between −0.5 and +0.5 at 25 and 27°C. In the room condition at 31°C, the all-air system has a lower thermal comfort level because the elevated airspeed is less effective when the mean radiant temperature (MRT) is low. This study suggests a cooling strategy to maximize the thermal comfort level by effectively utilizing the HRC in extreme conditions without extra cooling sources. When the designed set point indoor temperature is 25°C, the Airbox convector of the HRC fan can be off. However, if the indoor air temperature increases above 25°C, an occupant can activate the Airbox convector; the actual thermal output of HRC is increased, and the elevated airspeed can reduce the predicted percentage dissatisfied (PPD) level. Even in an extreme indoor thermal condition at 31°C, the HRC minimizes the PPD level.

Introduction

The building construction sector is mainly responsible for greenhouse gas emissions, as buildings have consumed around 40% of total primary energy and a related 40% of total greenhouse gas emissions.[1–3] Moreover, heating, ventilation and air conditioning (HVAC) systems result in the majority of energy consumption in buildings. Specifically, in residential and commercial buildings, an HVAC system is mainly responsible for energy consumption.[1,2] Compared with typical all-air systems, conventional radiant cooling systems have many advantages for buildings, such as less energy consumption, better thermal comfort, reduced air duct volume and relatively lower fan noise.[4–9] However, typical radiant cooling panel systems have some disadvantages using in buildings, following: (1) moisture condensation risk in an

[1]School of Thermal Engineering, Shandong Jianzhu University, Jinan, China
[2]Department of Civil Engineering and Energy Technology, Oslo Metropolitan University, Oslo, Norway
[3]Department of Mechanical Engineering, University of Maryland, College Park, MD, USA

Corresponding author:
Moon Keun Kim, Oslo Metropolitan University, P.O. Box 4, St. Olavs plass NO-0130 Oslo, Norway.
Email: Moon.Kim@oslomet.no; yan1492@gmail.com

especially hot and humid climate, (2) difficulties in adjusting the cooling output for a space zoning, (3) time delay to activate the radiant cooling system, and (4) a limitation of use in highly polluted indoor space, owing to lower air movement rates.[4,10–13] To overcome the downsides, a hybrid radiant cooling system (HRC) couples a conventional chilled water-based radiant panel with a compact Airbox convector consisting of heat exchangers, air fans, a water drain tube and an air filter. Kim and Leibundgut [6,14] designed the HRC system at the Swiss Federal Institute of Technology in Zurich . In the HRC system, a conventional radiant cooling panel and the compact Airbox convector are connected in series hydronically. This novel system can minimize the disadvantageous characteristics of the all-air and conventional radiant cooling (CRC) system and has several major benefits, including (1) reduction of vapour condensation risks, (2) enhancement of mixed convection effects by the Airbox fans, (3) minimization of the time delay to activate the system for thermal comfort, and (4) reduction of the indoor air pollutant concentrations by using an air filter.[6,15] Compared with a CRC system, the HRC system can save approximately 6–9% of the annual cooling energy consumption.[6] This is because the HRC system has a higher coefficient of performance (COP) of the cooling system and a higher cooling impact ratio compared to that of the CRC system, and it also offsets the rise in operative temperature by raising the indoor airflow.[6,16]

According to the literature, most evaluations of the three systems' energy performance (typical all-air system, CRC, and HRC) were compared and analysed while maintaining stable external and internal thermal environments.[5,6,17–21] However, still, now no research has illustrated performance of thermal comfort level of HRC system compared with two conventional systems. This study newly evaluates the performance of thermal comfort of three systems as a comparative analysis. Therefore, with numerical analysis, this study explores whether the HRC can be optimized in dynamic operational conditions, e.g., unexpected and extremely hot climates caused by an urban heat island and global warming effect. Significantly, this system can be rapidly adapted to extreme weather conditions and associated thermal loads. Hence, the study explores the amount of energy that is additionally consumed or saved, in comparison with the amount of energy required by other all-air systems and CRCs. Also, besides, if the system is unable to cool a room entirely, i.e., in a condition where the cooling loads are too high, the study also attempts to explore whether the system can adjust a space zoning to direct cooling to an occupied zone to maintain thermal comfort without additional cooling source or with a lower cooling energy inputs. Overall, this study aims to quantify the HRC's effects on thermal comfort and high-efficiency energy performance in extreme cooling load conditions. This study provides energy-saving strategies by using an HRC for maintaining thermal comfort in a building under challenging thermal conditions.

System setup

Building characteristics

We selected one small office using an air-source heat pump system centralized for cooling and dehumidification as a case study. The office building is placed in Shanghai, China, where the weather conditions in summer are hot and humid. Small office space was tested to calculate the cooling loads and dehumidification demand, and total cooling and ventilation energy consumption rates in a building. Figure 1 illustrates the annual weather data for Shanghai. In the summer (June–August), the temperatures and humidity ratios gradually increased, with the extreme conditions exceeding 35°C of air temperature and 25 g/kg of humidity ratio. Therefore, buildings in Shanghai have high cooling and dehumidification loads. The office wall materials were selected and simulated in two scenarios: one with general wall material insulation following Chinese building construction regulations for hot summer and cold winter seasons and good performance insulation, such as insulation having a low U-value. The building boundary condition is shown in Table 1. The short wall of the building faces east and west. The thermal energy loads for cooling were simulated by TRNSYS software modelling.[22] Table 2 shows U-values of the building materials. The insulation strategy was categorized into two parts: normal insulation and good insulation. The U-values of normal insulation were satisfied with the standard requirement in China,[23] and the U-values of good insulation were suggested for saving thermal energy consumption in a building. This study used a supply airflow rate for the office room, based on the standard, American Society of Heating, Refrigerating and Air-Conditioning Engineers (ASHRAE) 62.1–2014.[24] Figure 2 shows the geometry of a small office room and the positions L1, L2 and L3 represent the windows side, middle area and internal wall area in an office room. The height of the three positions is 1.2 m from the floor. The distance of L1 and L3 from the windows and internal wall is 1 m. L2 is posited at the centre. The thermal performance at these positions can illustrate how radiant surface temperature, wall surface areas, air temperature and air velocity influence the positions' thermal comfort level as a comparative analysis. The boundary conditions are shown in Table 1.
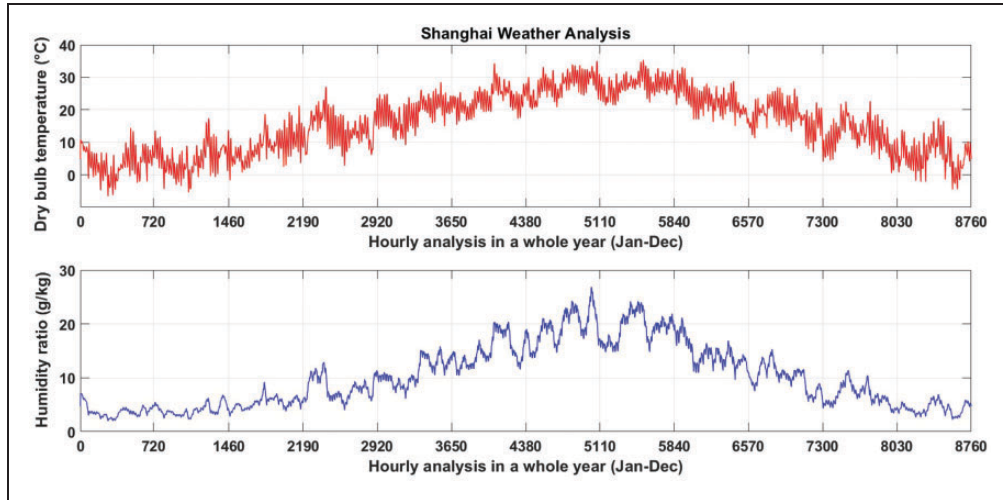
Figure 1. Weather data for Shanghai.

Table 1. Designed boundary conditions and geometry of a small office room.

Office volume (m^3)	42.8
Net space area (m^2)	14.8
Wall height (m)	2.896
Long wall width (m)	6.058
Short wall with (m)	2.438
Windows height (m)	1.4
Windows width (m)	1.43
Air infiltration rate (ACH)	0.1
Occupant activity (W)	100
Office equipment (W)	230
Artificial lighting (W/m^2)	5

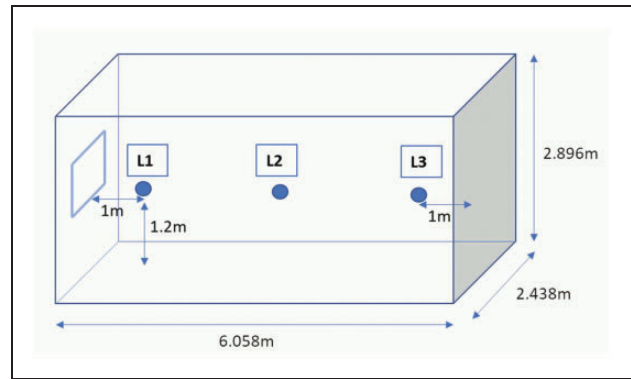**Figure 2.** Geometry of a small office room.

Table 2. U-values of each wall, ceiling and floor.

Structure	Area (m^2)	U-values (W/m^{2}K) Normal insulation	U-values (W/m^{2}K) Good insulation
Ceiling	14.76	0.298	0.129
Long walls	17.54	0.356	0.129
Short walls	7.06	0.356	0.129
Floor	14.76	0.040	0.040
Window	2	2.54	1.01

Cooling systems

In general, active cooling systems in a building can be categorized into three mechanical system types: all-air system, CRC and HRC systems, as illustrated in Figure 3. The all-air system is quite common and is widely used today. The system requires supplying a huge volume of air and consumes high fan energy, and further requires a large space to install the air duct system. The system supplies an amount of chilled and dehumidified air for cooling and ventilation, which includes 30% of air (fresh outdoor air, 1.0 air changes per hour (ACH)) and 70% of air (air recirculation, 2.0 ACH). This system delivers a large amount of air volume, and it consumes high fan energy, and releases relatively high airflow noise compared with a radiant cooling system with the displacement ventilation system. The energy efficiency of CRC is relatively higher than those of a typical all-air system. It is divided into the sensible cooling and air dehumidification works of the air conditioning process and minimizes the supply air volume and volume of space required for system devices. Hence, a radiant cooling system can minimize air pressure loss and save cooling energy in a building, owing to the highest-temperature cooling as a low exergy technology. However, it has high risks of vapour condensation risk on the radiant cooling surface when high internal
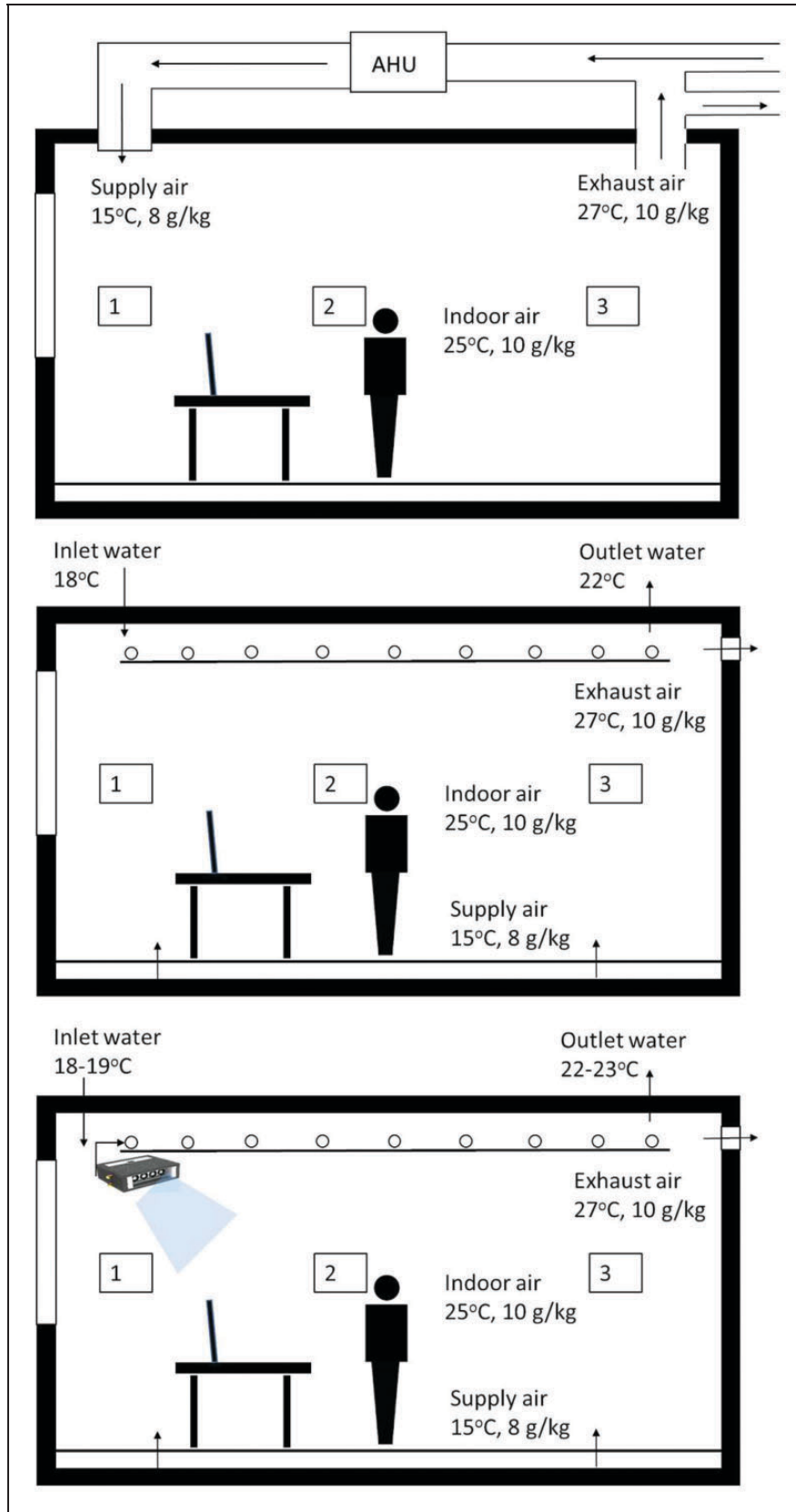
Figure 3. Schematic diagram of three main systems and positions, L1, L2 and L3: typical all-air system (top), conventional radiant cooling panel (CRC) system (middle) and novel hybrid radiant cooling panel system with Airbox convector (HRC) (bottom).

moisture gains and infiltration increase the indoor humidity level, particularly in hot and humid ambient air conditions. In order to reduce the condensation risk, the system must dehumidify the supply airflow by a specific air humidity ratio of 8 g/kg. Moreover, it has slow air movement compared to the air movement of all-air systems. Thus, it has difficulties in reducing indoor air pollutant concentrations when the indoor space is seriously polluted. An HRC system and its performance are also illustrated in Figure 2. Kim and Leibundgut [14] designed the HRC system not only to prevent moisture condensation risk on the surface of the chilled radiant panel, but also to generate additional cooling output with enhanced mixed convection effect by compact airbox heat exchangers and fans. This system is composed of two devices. One is a conventional chilled water radiant cooling panel system, and the other is a compact Airbox convector consisted of heat exchangers, air filter and fan. These two devices are hydronically coupled in series.

Figure 4 illustrates an Airbox composed of compact heat exchangers, fans, air filters, water pipes, a power adapter, controller and a drain tube. As a main cooling energy source, the supplied chilled water passes through the Airbox convector's heat exchangers and then flows through the radiant ceiling panel. If the Airbox unit is off, the system performance is the same as a conventional radiant cooling system. The capacity of a typical Airbox cooling out is around 161–752 W per unit tested depending on supply air temperature and water flow rates and air resistance of the filter system is approximately 250–450 Pa.[25] Indoor air humidity ratio can be adjusted by the Airbox convector, and the moisture is condensed in the Airbox convector when the indoor humidity ratio is exceeded to higher than 12 g/kg specific humidity ratio, and it increases the supply water temperature toward the radiant cooling panel, owing to the thermal heat transfer in the compact Airbox heat exchangers.[6,26]
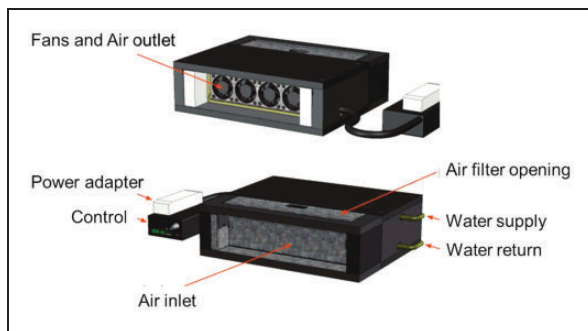

Figure 4. Airbox unit and compositions, BS2 AG, Switzerland.[25]

Indoor environment to adapt to extreme condition

According to literature,[5,11,12,27–31] the CRC has problems in extremely hot and humid climates. In order to increase cooling output using a conventional radiant cooling panel system in especially tropical or hot and humid weather conditions, the lower temperature supply water needs, but it causes the higher vapour condensation risk. For example, if one-day cooling loads are too high owing to an extreme weather condition or high indoor heat gains, and the indoor operative temperature is higher than 27°C, the radiant cooling system has difficulty in increasing the cooling output and cooling the entire space with the lower supply water temperature below 16°C. However, an HRC can simply adjust the cooling output, owing to the enhanced additional mixed convection effect by the Airbox convector. The increase in air movement helps improve the indoor thermal comfort level. Also, the ASHRAE standard 55 [32] allows for an elevated indoor airflow speed limited to 0.8 m/s and 1.2 m/s depending on with or without local control to be used to increase the operative temperature, for operative temperatures higher 25.5°C. Therefore, the HRC can maximize the operative temperature by using the Airbox convector to enhance the mixed convection effect and can save additional cooling energy consumption in buildings in extreme conditions.[6] Moreover, it can simplify indoor space zoning with air movement and directivity changes to adapt to occupants' variable thermal preferences. This study considers the potential amount of cooling energy that can be saved to maximize the operative temperature in extreme conditions, with and without local airspeed control from an Airbox convector.

Cooling energy analysis

The cooling energy consumption and actual capacity of the systems are determined from the following equations.

The typical all-air system is described by equation (1)

$$Q_{all_{air}} = m_{supply.air}(h_{mix.air} - h_c) + m_{supply.air}C_{p.air}(T_{reheat} - T_c) \quad (1)$$

The CRC with a typical air handling unit (AHU) is expressed by equation (2)

$$Q_{typi_{radi_{AHU}}} = m_{rec.supply.\ air}(h_{out} - h_c) + m_{supply.air}C_p(T_{reheat} - T_c) + m_{supply.water}C_{p.water}(T_{out} - T_{in}) \quad (2)$$

where Q is the cooling energy consumption or output in W/m^2, m is the mass flow rate in kg/m^3, h is the enthalpy value in kJ/kg, C_p is the specific heat capacity of air and water in kJ/kg, T is the temperature in K and c is the chilled.

The HRC with AHU is determined by equation (3)

$$Q_{hybrid_{radiant_{airbox}}} = m_{rec.supply.air}(h_{out} - h_c) \\ + m_{supply.water}C_{p.water}(T_{out} - T_{in}) \\ + Q_{airbox.fan.energy} \quad (3)$$

The fan energy consumption is determined by equation (4)

$$fan\ energy\ (W) = \frac{V\Delta p}{3600\eta_f} \quad (4)$$

where fan energy is a parameter of the electric power, Watt, V is the volumetric airflow rate (m^3/h), Δp is the total pressure differences (Pa), and η_f is the fan efficiency of units.

The actual cooling output of the typical all-air and CRC are described by equations (5) and (6) as follows

$$Q_{c.c.all_{air}} = m_{supply.air}\left(h_{indoor.air} - h_{supply.air}\right) \quad (5)$$

$$Q_{c.c.typi_{radi}AHU} = m_{rec.supply.air}\left(h_{indoor.air} - h_{supply.air}\right) \\ + m_{supply.water}C_{p.water}(T_{out} - T_{in}) \quad (6)$$

The actual cooling outputs of HRC (CRC + Airbox convector) are described by equation (7)

$$Q_{c.c.hybrid_{radi}AHU} = m_{supply.\ air}\left(h_{indoor.air} - h_{supply.air}\right) \\ + m_{supply.water}C_{p.water}(T_{out} - T_{in}) \quad (7)$$

Kim et al.[6,33] proposed an equation, an actual cooling impact ratio for three main cooling systems. Equations (8), (9) and (10) defines the ratio between the actual cooling outputs and total cooling energy consumption of the all-air system and typical and hybrid radiant cooling panel system.

$$CCR_{All-air\ system} = \frac{Q_{c.c.all_{air}}}{Q_{all\ air}} \quad (8)$$

$$CCR_{Conv.radiant} = \frac{Q_{c.c.typi_{radi}AHU}}{Q_{typi_{radi}AHU}} \quad (9)$$

$$CCR_{Hybrid.radiant} = \frac{Q_{c.c.hybrid_{radi}AHU}}{Q_{hybrid_{radiant}airbox}} \quad (10)$$

According to Kim et al.,[34] the HRC shows the most energy-efficient performance with the highest impact ratio; however, the all-air system has relatively the lower cooling impact ratios. The HRC's cooling impact ratio was about 0.718, CRC's was 0.698 and the all-air system's impact ratio was 0.4. Based on boundary conditions with Shanghai summer weather condition and the system performance using equations (7) to (9), the impact ratios of the three systems were newly calculated. The all-air system had cooling impact ratios around 0.51–0.65. The CRCs were around 0.76–0.90 and the HRCs were around 0.78–0.96. Thus, the HRC's cooling impact ratios are higher than those of CRC and all air system.

Mixed convection effect

Beausoleil-Morrsion[35] built heat transfer correlations of mixed convection using Churchill and Usagi's[36] and Alamdaris and Hammond's[37] approaches. Awbi and Hatton[38] defined the coefficients of mixed convection heat transfer. Jeong and Mumma[39,40] proposed simplified cooling capacity estimation modelling using mixed convection coefficient, and the equations for calculating the cooling capacity of a radiant cooling panel with mixed convection are described in equations (11) to (18)

$$q_o = q_c - q_r \quad (11)$$

$$q_c = ht_c(T_a - T_{pm}) \quad (12)$$

$$q_r = ht_r(AUST - T_{pm}) \quad (13)$$

$$Oc = \frac{q_o}{T_a - T_{pm}} \quad (14)$$

$$Oc = \frac{q_c + q_r}{(T_a - T_{pm})} = ht_c + ht_r\frac{AUST + T_{pm}}{(T_a - T_{pm})} \quad (15)$$

$$ht_r = 5 \times 10^{-8}\left[(AUST + 273)^2 + (T_{pm} + 273)^2\right] \\ \left[(AUST + 273) + (T_{pm} + 273)\right] \quad (16)$$

$$ht_c = F_c + 2.13\ \Delta T^{0.31} \quad (17)$$

$$F_c = \alpha_0 + \alpha_1(\Delta T) + \alpha_2(V) + \alpha_3(W) + \alpha_4(V \cdot W) \quad (18)$$

where q is the heat flux to the panel in W/m^2, O is the total, c is the convection, r is the radiation, ht is the heat transfer coefficient (W/m^{2}K), $AUST$ is the area-weighted average temperature in °C, T_{pm} is the panel

mean surface temperature in °C, *a* is air, F_c is a correction function (W/m²K), *V* is the diffuser air velocity (m/s) and *W* is the width of the nozzle diffuser
where

α_0	α_1	α_2	α_3	α_4
0.28021	−0.13931	0.11416	1.25013	1.22058

Kim and Leibundgut[26] proposed a capacity of the HRC that combines the mixed convection effect of the CRC system with the Airbox convector's cooling capacity. The total cooling capacity of the HRC is shown by equation (19) below

$$O_t = O_c + m_{\text{supply.water in Airbox}}\ C_{p.water}(T_{out} - T_{in})$$
(19)

where O_t is the total cooling capacity of the HRC (W/m²K).

Kochendörfer[41] described that the air diffuser's indoor air velocity increases 10–15% of the actual radiant cooling output with mixed convection effect. Jeong and Mumma[39] stated that the mixed convection effect could improve cooling output around 10–39%, depending on the material heat coefficient. Kim and Leibundgut[26] showed that the total cooling output of the HRC could be improved by approximately 32% in comparison with the CRC. Hence, the Airbox convector's airflow generation enhances the mixed convection effect, and the heat transfer coefficient of the heat exchangers in the Airbox generates extra cooling output. This study used the results of the mixed convection effect by Jeong and Mumma[39] and the results regarding the HRC's capacity by Kim and Leibundgut [15] to define the actual cooling output of the systems.

Evaluation of PMV and PPD model

In terms of presenting potential of the cooling systems, this study also evaluated the performance of satisfying thermal comfort, predicted percentage dissatisfied (PPD) models and predicted mean vote (PMV), and of an HRC, in comparison with an all-air system and a CRC. In terms of the indoor thermal comfort performance, we used PPD and PMV indexes following the international standard ISO 7730.[42] The main parameters describe occupants' thermal satisfaction from variable perspectives.

Main factors in determining PMV and PPD value consist of indoor air temperature (°C), air velocity (m/s), humidity ratio (g/kg), mean radiant temperature (MRT) (°C), activity (metabolic) and the occupant's clothing (clo). The PMV index achieves thermal satisfaction ranges in a scale value from cold and hot references and a range for a comfortable indoor space environment. With regard to the PPD index, the PPD must be controlled to be under 10% to achieve a general thermal comfort level (ASHRAE).[32] The PMV value was determined by equations (20) to (23). The PPD value was evaluated by equation (24). The MRT is a crucial element influencing occupants' thermal comfort level. Regarding the calculation of the MRT at a position in a room, this study defined an ambient outside air temperature of 30–35°C considered as extreme climates. Based on the characteristics of boundary conditions, wall materials, thermal conductivity, thickness and temperature gradient, the indoor wall surface temperature exposed to the external wall was 27–31°C, with an indoor dry bulb temperature of 25–31°C.[43] The detailed conditions of surface temperatures of the external and internal walls, ceiling and floor surface are listed in Table 3.

$$
\begin{aligned}
PMV = {}& \left[0.303 \times \exp(-0.036 \times M) + 0.028\right] \\
& \times \big\{(M - W) - 3.05 \times 10^{-3} \\
& \times \left[5733 - 6.99 \times (M - W) - p_a\right] - 0.42 \\
& \times \left[(M - W) - 58.15\right] - 1.7 \times 10^{-5} \\
& \times M \times (5867 - p_a) - 0.0014 \times M \\
& \times (34 - t_a) - 3.96 \times 10^{-8} \times f_{cl} \\
& \times \left[(t_{cl} + 273)^4 - (\bar{t}_r + 273)^4\right] - f_{cl} \times h_c \\
& \times (t_{cl} - t_a)\big\}
\end{aligned}
$$
(20)

$$
\begin{aligned}
t_{cl} = {}& 35.7 - 0.028 \times (M - W) - I_{cl} \\
& \times \big\{3.96 \times 10^{-8} \times f_{cl} \times \left[(t_{cl} + 273)^4 - (\bar{t}_r + 273)^4\right] \\
& + f_{cl} \times h_c \times (t_{cl} - t_a)
\end{aligned}
$$
(21)

$$
h_c = \begin{cases} 2.38 \times t_{cl} - t_a{}^{0.25} \ \text{for}\ 2.38 \times |t_{cl} - t_a{}^{0.25} > 12.1 \times \sqrt{v_{ar}} \\ 12.1 \times \sqrt{v_{ar}} \ \text{for}\ 2.38 \times |t_{cl} - t_a{}^{0.25} < 12.1 \times \sqrt{v_{ar}} \end{cases}
$$
(22)

Table 3. Designed surface temperatures of wall, ceiling and floor.

Structure	Area, m²	All-air, °C	CRC, °C	HRC, °C
External wall	7.06	28–31	28–31	28–31
Internal wall	42.14	25–28	25–28	25–28
Ceiling	42.8	27–29	20–22	21–23
Floor	42.8	23–25	23–25	23–25

$$f_{cl} = \begin{cases} 1.00 + 1.290 \times I_{cl} \ for \ I_{cl} \leq 0.078 \, \mathrm{m^2K/W} \\ 1.05 + 0.645 \times I_{cl} \ for \ I_{cl} > 0.078 \, \mathrm{m^2K/W} \end{cases}$$

$$(23)$$

where

t_a is the air temperature (°C);

$\bar{t}_r$ is the MRT, in degrees Celsius (°C);

t_{cl} is the clothing surface temperature (°C).

M is the metabolic rate (W/m^2);

W is the effective power (W/m^2);

I_{cl} is the clothing insulation (m^2 K/W);

f_{cl} is the clothing surface area factor;

v_{ar} is the relative air velocity (m/s);

p_a is the water vapour partial pressure (Pa);

h_c is the convective heat transfer coefficient (W/m^{2}K); and

$$PPD = 100-95 \ \exp(-0.03353 \ PMV^4-0.2179 \ PMV^4)$$

$$(24)$$

where

PMV is the predicted mean vote;

PPD is the predicted percentage dissatisfied (%)

ASHRAE fundamentals[44] and International standard ISO 7730[42] indicate the method to calculate the mean radiant temperature (MRT). The surface temperatures of the ceiling, walls and floor and the angle factors affect mean radiant temperature as described in equation (25)

$$MRT^4 = T^4_1 F_{p-1} + T^4_2 F_{p-2} + \cdots + T^4_n F_{p-n} \qquad (25)$$

In the above equation

F_{p-n} is the angle factor between a surface and an occupant;

T_n is the temperature of surface 'n' (K)

Results and discussion

Numerical cooling load analysis

To analyse the cooling load in a building, we used the TRNSYS building energy simulation software [22] based on four main conditions: a normal insulated room with and without internal heat obtained and a well-insulated room with and without internal heat gain. Figure 5 illustrates the cooling demand of the office room. As illustrated in Figure 5, the thermal resistance of building envelopes and internal heat gains highly impacted on thermal energy consumption. The well-insulated space can save around 30% of cooling energy consumption compared with a normal wall insulation condition. Moreover, internal heat gains also significantly influence total cooling energy.

As illustrated in Figures 6 and 7, the CRC generally provides sufficient cooling outputs considering two conditions, normal and well-insulated room with steel and aluminium panels, using 18–19°C of supply water temperature. In extreme outdoor weather conditions, the generated cooling output is not sufficient to eliminate the cooling load. The conventional approach to increase the cooling capacity of the CRC is to decrease the supply water temperature passing through the
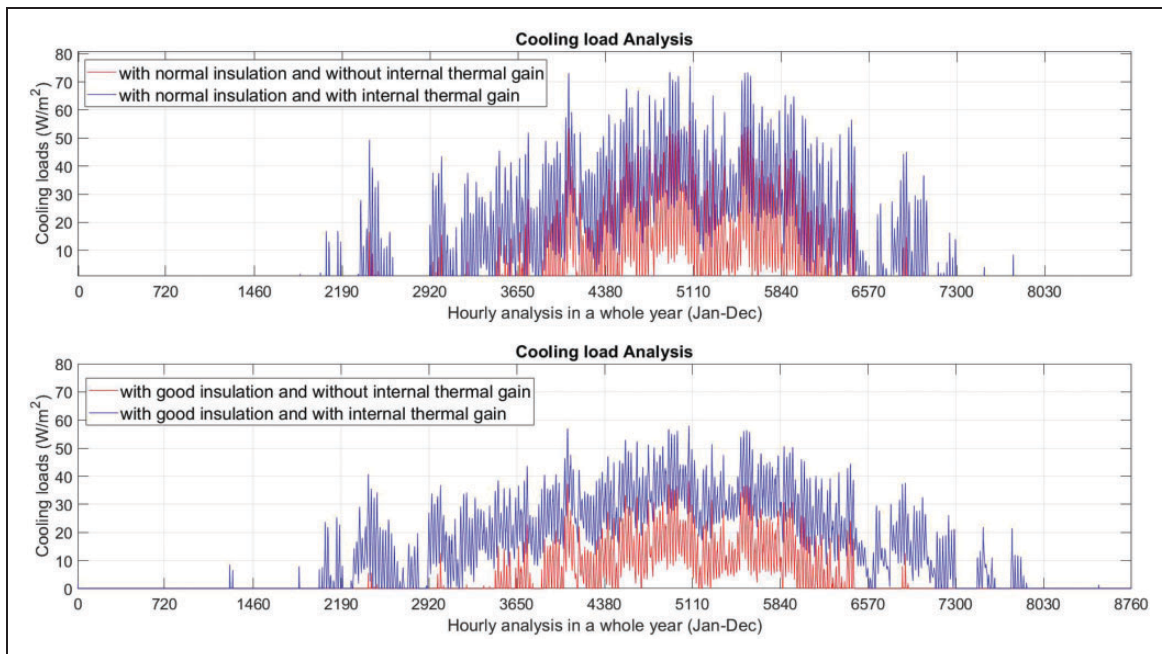

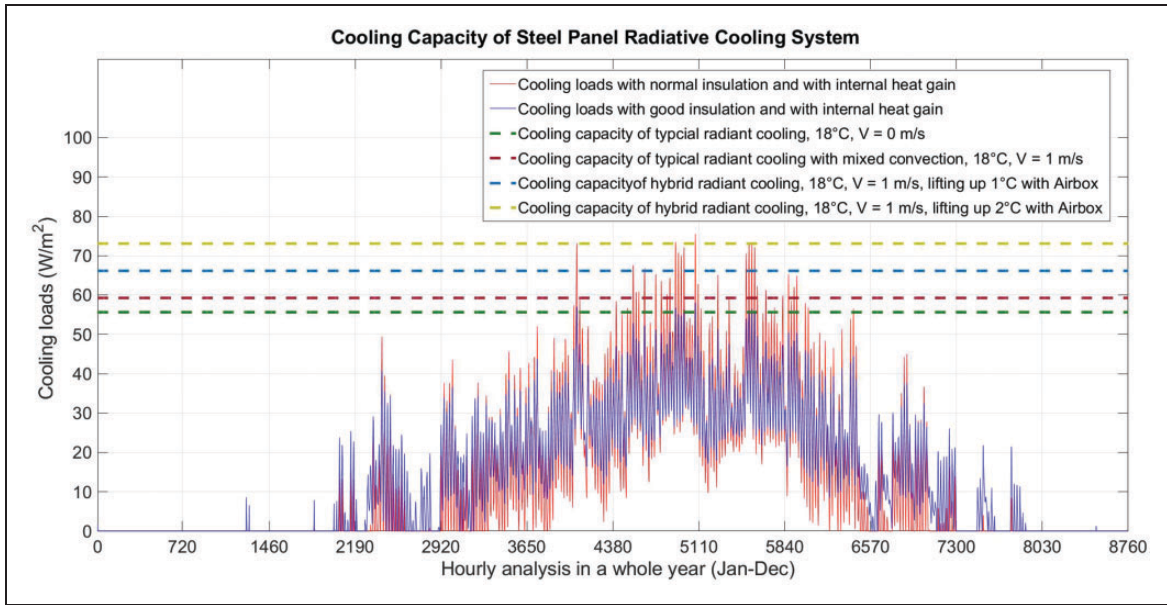**Figure 5.** Cooling loads of the designed room.

Figure 6. Cooling loads of the design room and cooling output of typical and hybrid steel radiant cooling panel system with 18°C of supply water temperature.
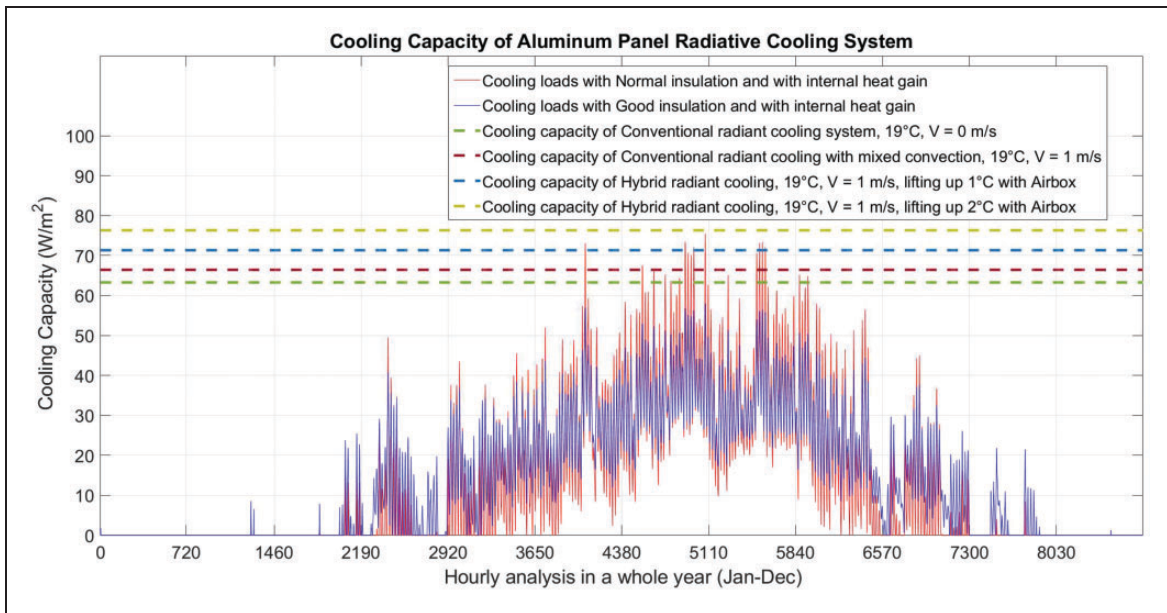

Figure 7. Cooling loads of the design room and cooling output of typical and hybrid aluminium radiant cooling panel system with 19°C of supply water temperature.

chilled cooling panel. However, it is quite limited in use, as lower-temperature cooling causes a high moisture condensation risk in hot and humid weather conditions. Moreover, it is also challenging to supply water with different temperatures in rooms while considering varied thermal load demands. Figures 6 and 7 illustrate the reasons why the HRC can be well-optimized for adapting to varied thermal room conditions. The HRC can simply adjust the cooling capacity by

Airbox fan controls with a mixed convection effect. The results illustrate the significant differences between CRC and HRC. Even if both systems generate the same cooling outputs, the HRC can save around 5% of energy consumption compared with the CRC, because the HRC shows efficient energy performance with higher actual cooling impact values, and a higher temperature cooling system has higher COP values.[6] Kim et al.[6] investigated that HRC system can save a

total of 9.3% of the cooling energy compared with the CRC system due to the higher coefficient of performance of the Chiller system as a lower exergy technology and higher cooling impact ratio. Figures 6 and 7 illustrate the advanced cooling strategy using the HRC. When the thermal load in a room is lower than the CRC's cooling capacity, we can turn off the Airbox system of the HRC, as utilization of the CRC. However, once the indoor thermal loads are higher than the CRC's capacity, e.g., in an extreme weather condition, then we turn on the Airbox system with fan control and adjust the cooling performance. The Airbox convector enhances the mixed convection effect, as well as the heat exchangers generate extra cooling output. Therefore, the increased capacity of the HRC covers the increased cooling load in the room without adding an extra cooling source.

Thermal comfort analysis using three cooling systems

Tables 4 to 6 list the indoor conditions and main elements of PPD and PMV with room temperatures of 25°C, 27°C and 31°C using three main cooling systems: the all-air system, CRC and HRC. The locations L1, L2 and L3 are illustrated in Figure 2.

Figures 8 and 9 illustrate the impacts of elevated air movement and MRT on thermal comfort, PMV and PPD at the same cooling outputs of three cooling strategies. The ASHARE standard 55[16] describes the requirement that can adjust elevated air velocity to maximize the operative temperature to design a comfort zone. Mumma [45] described that a room condition at 25.6°C with chilled water radiant panel system can achieve a perception of a condition at 23.9 °C without radiant panels. Thus, a chilled radiant panel system can expand comfort temperature range in a psychrometric chart compared with all air system. As a thermal comfort comparison, the literature[45–49] shows that radiant cooling ceiling panels presented a better performance than all-air systems based on occupant response and laboratory outcomes. However, some literature suggests no specific preferences found between the two systems.[50–53] The results in Figures 8 and 9 illustrate the thermal performances of the three cooling systems. The all-air system and CRC have no specific large differences at the temperatures of 25–27°C, because at 25–27°C, the PMV values are predicted near the thermal comfort zone, ±0.5. However, the CRC has a slightly better thermal comfort at a relatively lower temperature of 25°C and the all-air system has a slightly superior comfort at 27°C.

Table 4. Indoor conditions and main elements of predicted percentage dissatisfied (PPD) and predicted mean vote (PMV) with indoor dry bulb temperature 25°C and humidity ratio 10 g/kg.

	Unit	L1	L2	L3
All-air system				
Indoor dry bulb temperature	°C	25	25	25
Mean radiant temperature	°C	26	25.63	25.44
Air velocity	m/s	0.3	0.3	0.3
Clothing	Clo	0.5	0.5	0.5
Activity	Met	1.2	1.2	1.2
PMV		−0.23	−0.28	−0.31
PPD	%	6.1	6.6	6.9
CRC				
Indoor dry bulb temperature	°C	25	25	25
Mean radiant temperature	°C	24.61	23.75	24.06
Air velocity	m/s	0.1	0.1	0.1
Clothing	Clo	0.5	0.5	0.5
Activity	Met	1.2	1.2	1.2
PMV		0	−0.13	−0.08
PPD	%	5	5.3	5.1
HRC				
Indoor dry bulb temperature	°C	25	25	25
Mean radiant temperature	°C	24.89	24.13	24.33
Air velocity	m/s	0.2	0.3	0.15
Clothing	Clo	0.5	0.5	0.5
Activity	Met	1.2	1.2	1.2
PMV		−0.21	−0.47	−0.18
PPD	%	5.9	9.7	5.7

Table 5. Indoor conditions and elements of PPD and PMV with indoor dry bulb temperature 27°C and humidity ratio 10 g/kg.

	Unit	L1	L2	L3
All-air system				
Indoor dry bulb temperature	°C	27	27	27
Mean radiant temperature	°C	28	27.63	27.44
Air velocity	m/s	0.3	0.3	0.3
Clothing	Clo	0.5	0.5	0.5
Activity	Met	1.2	1.2	1.2
PMV		0.44	0.39	0.36
PPD	%	9	8.1	7.7
CRC				
Indoor dry bulb temperature	°C	27	27	27
Mean radiant temperature	°C	26.61	25.75	26.06
Air velocity	m/s	0.1	0.1	0.1
Clothing	Clo	0.5	0.5	0.5
Activity	Met	1.2	1.2	1.2
PMV		0.57	0.44	0.49
PPD	%	11.7	9	9.9
HRC				
Indoor dry bulb temperature	°C	27	27	27
Mean radiant temperature	°C	26.89	26.13	26.33
Air velocity	m/s	0.2	0.3	0.15
Clothing	Clo	0.5	0.5	0.5
Activity	Met	1	1	1
PMV		0.42	0.19	0.42
PPD	%	8.6	5.7	8.7

Table 6. Indoor conditions and elements of PMV and PPD with indoor dry bulb temperature 31°C and humidity ratio 10 g/kg.

|	Unit	L1	L2	L3
All-air system				
Indoor dry bulb temperature	°C	31	31	31
Mean radiant temperature	°C	30.19	29.88	29.36
Air velocity	m/s	0.3	0.3	0.3
Clothing	Clo	0.5	0.5	0.5
Activity	Met	1	1	1
PMV		1.53	1.49	1.42
PPD	%	52.6	50.3	46.6
CRC				
Indoor dry bulb temperature	°C	31	31	31
Mean radiant temperature	°C	28.81	28	27.97
Air velocity	m/s	0.1	0.1	0.1
Clothing	Clo	0.5	0.5	0.5
Activity	Met	1	1	1
PMV		1.43	1.31	1.31
PPD	%	47.3	40.8	40.8
HRC				
Indoor dry bulb temperature	°C	31	31	31
Mean radiant temperature	°C	29.08	28.28	28.25
Air velocity	m/s	0.8	1.2	0.6
Clothing	Clo	0.5	0.5	0.5
Activity	Met	1	1	1
PMV		1.28	1.15	1.21
PPD	%	39.2	32.8	35.8
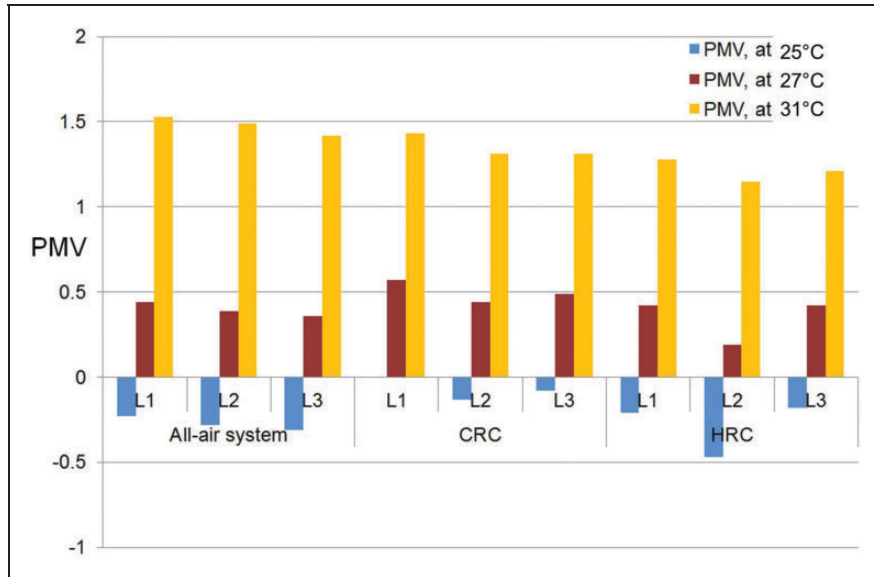
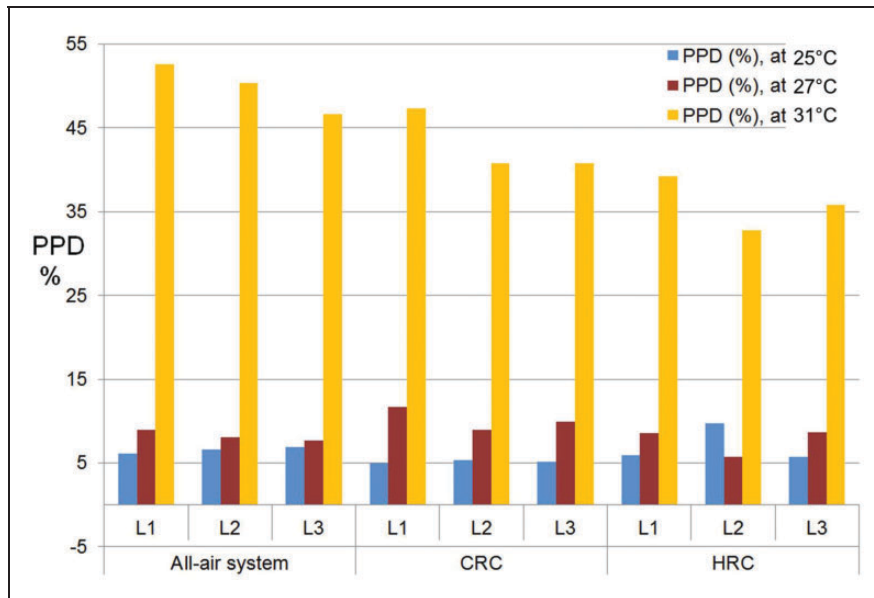**Figure 8.** Parameters of predicted mean vote (PMV) at indoor temperatures of 25°C, 27°C and 31°C.

Figure 9. Parameters of the predicted percentage dissatisfied (PPD) at indoor temperatures of 25°C, 27°C and 31 °C.

This study also includes a thermal comfort analysis for spaces cooled by HRC. In the room condition at 25°C, the CRC system shows better thermal comfort conditions than those of others' system because the elevated airspeed in the typical all-air system and HRC makes a draft. At the room condition at 27°C, the high airspeed from the all-air system and HRC offset the rise in the indoor temperature and improve thermal comfort level as measured by PMV/PPD. In particular, HRC can simplify thermal space zoning, owing to airspeed and directivity control by the Airbox convector unit. The three systems perceive thermal comfort in PMV between –0.5 and +0.5 at 25 and 27°C. In the room condition at 31°C, the all-air system has a lower thermal comfort level, because the elevated airspeed is less effective when the MRT is lower and the indoor temperature is increased.[16] Figures 8 and 9 illustrate a cooling strategy to maximize the thermal comfort level by utilizing the HRC effectively. When the designed set point indoor temperature is 25°C, the Airbox convector of the HRC fan can be off. However, if the indoor air temperature is increased

above 25°C, an occupant can activate the Airbox convector; the actual cooling output of HRC is increased, and the elevated airspeed can reduce the PPD level. Even in an extreme indoor thermal condition at 31°C, the HRC minimizes the PPD level, owing to the CRC's combination and the mixed-air convection effect by the Airbox convector. Thus, the HRC effectively adapts to extremely hot and dry or hot and humid conditions because the compact Airbox system simply adjusts the cooling outputs due to the elevated airspeed and mixed convection effect and improves indoor thermal comfort. Nevertheless, a limitation remains to be investigated via additional studies. This study did choose an office room to evaluate thermal load and comfort, focusing on cooling system types and PMV/PPD modelling. However, as the vertical temperature gradient and ventilation types impact the actual thermal comfort, a future study should consider investigating the performance with experimental methods.

Conclusion

This study examined a novel HRC system and evaluated its performance compared with the conventional all-air and CRC systems by numerical analysis. Detailed numerical calculations of cooling outputs and thermal comfort levels demonstrated the HRC system's ability to adapt to extremely hot and humid conditions and associated thermal loads. In fact, the studied HRC system has higher cooling capacity compared to conventional systems, owing to the enhanced mixed convection effect and additional cooling outputs from the Airbox convector. The conventional CRC system has an operational limitation in extreme weather, especially hot and humid conditions. Their lower supplying chilled water temperature can cause water vapour condensation on the surfaces of chilled panels. Therefore, these conventional systems have difficulties in maintaining thermal comfort during extreme weather conditions. Importantly, the studied HRC system can adjust the cooling output and provide excellent thermal environment using the Airbox convector even during extreme weather conditions without additional cooling sources added. This feature of the HRC systems has additional benefits in allowing flexible cooling outputs to adapt to extreme weather conditions. In particular, HRC can simplify thermal space zoning, owing to airspeed and directivity control by the Airbox convector unit. The three systems perceive thermal comfort in the predicted mean vote (PMV) between –0.5 and +0.5 at 25 and 27°C. In the room condition at 31°C, the all-air system has a lower thermal comfort level because the elevated airspeed is less effective when the mean radiant temperature (MRT) is lower, and the indoor temperature is increased.

The HRC achieves better thermal comfort levels when the indoor temperature is higher than a normal thermal comfort-zone temperature, compared to the thermal comfort levels with the conventional all-air and CRC systems. Overall, the HRC system can improve indoor thermal comfort and simplify space zoning with the variable air volume control and directivity provided by the Airbox convector. This study demonstrated that the HRC could reliably provide cooling in the hot summer season, especially in areas highly affected by climate change and global warming.

ORCID iDs

Jiying Liu https://orcid.org/0000-0001-7385-6959
Moon Keun Kim https://orcid.org/0000-0001-9614-5412

References

1. de Ia Rue Du Can S and Price L. Sectoral trends in global energy use and greenhouse gas emissions. *Energ Policy* 2008; 36: 1386–1403.
2. Agency IIE. *Promoting energy efficiency investments: case studies in the residential sector*. Paris Cedex 15: OECD/IEA and AFD, 2008.
3. Programme UNE. *Buildings and climate change*. Paris CEDEX09, France: United Nations Environment Programme, 2009.
4. Zhang LZ and Niu JL. Indoor humidity behaviors associated with decoupled cooling in hot and humid climates. *Build Environ* 2003; 38: 99–107.
5. Novoselac A and Srebric J. A critical review on the performance and design of combined cooled ceiling and displacement ventilation systems. *Energ Build* 2002; 34: 497–509.
6. Kim MK, Liu JY and Cao SJ. Energy analysis of a hybrid radiant cooling system under hot and humid climates: a case study at Shanghai in China. *Build Environ* 2018; 137: 208–214.

7. Novoselac A, Burley BJ and Srebric J. New convection correlations for cooled ceiling panels in room with mixed and stratified airflow. *HVAC&R Res* 2006; 12: 279–294.

8. Lv G, Shen C, Han Z, Liao W and Chen D. Experimental investigation on the cooling performance of a novel grooved radiant panel filled with heat transfer liquid. *Sustain Cities Soc* 2019; 50: 101638.

9. Xie D, Wang CH, Yu CW, Wang Y and Wang HQ. Performance of capillary ceiling cooling panel on ceiling surface temperature and indoor thermal environment. *Indoor Built Environ*. 2020; 29: 881–894.

10. Niu JL, Zhang LZ and Zuo HG. Energy savings potential of chilled-ceiling combined with desiccant cooling in hot and humid climates. *Energy Build* 2002; 34: 487–495.

11. Kim T, Kato S, Murakami S and Rho J. Study on indoor thermal environment of office space controlled by cooling panel system using field measurement and the numerical simulation. *Build Environ* 2005; 40: 301–310.

12. Hu R and Niu JL. A review of the application of radiant cooling & heating systems in Mainland China. *Energy Build* 2012; 52: 11–19.

13. Zhao WZ, Kilpelainen S, Kosonen R and Jokisalo J. Experimental comparison of local low velocity unit combined with radiant panel and diffuse ceiling ventilation systems. *Indoor Built Environ* 2020; 29: 895–914.

14. Kim MK and Leibundgut H. Evaluation of the humidity performance of a novel radiant cooling system connected with an Airbox convector as a low exergy system adapted to hot and humid climates. *Energ Build* 2014; 84: 224–232.

15. Kim MK and Leibundgut H. A case study on feasible performance of a system combining an Airbox convector with a radiant panel for tropical climates. *Build Environ* 2014; 82: 687–692.

16. ANSI/ASHRAE Standard 55-2010. *Thermal environmental conditions for human occupancy*. Atlanta: The American Society of Heating, Refrigerating and Air Conditioning Engineers, 2010.

17. Kim KW and Olesen BW. Radiant heating and cooling systems. *ASHRAE J* 2015; 57: 28–37.

18. Liu J, Dalgo DA, Zhu S, Li H, Zhang L and Srebric J. Performance analysis of a ductless personalized ventilation combined with radiant floor cooling system and displacement ventilation. *Build Simul* 2019; 12: 905–919.

19. Gao S, Li Y, Wang YA, Meng XZ, Zhang LY, Yang C and Jin LW. A human thermal balance based evaluation of thermal comfort subject to radiant cooling system and sedentary status. *Appl Therm Eng* 2017; 122: 461–472.

20. Lim H, Kang Y-K and Jeong J-W. Thermoelectric radiant cooling panel design: numerical simulation and experimental validation. *Appl Therm Eng* 2018; 144: 248–261.

21. Cao SJ, Yu CW and Luo XL. Heating, ventilating and air conditioning system and environmental control for wellbeing. *Indoor Built Environ* 2020; 29: 1191–1194.

22. TRNSYSTRNSYS Transient System Simulation Tool. *TRNSYS 18 ed*. Madison WI: Thermal Energy System Specialists, LLC, 2018.

23. Shui B, Evans M, Lin H, Jiang W, Liu B, Song B and Somasundaram S. *Country report on building energy codes in China*. Washington,: Pacific Northwest National Laboratory, United States Department of Energy, 2009.

24. ASHRAE Standard 62.1-2010. *Ventilation for acceptable indoor air quality*. Atlanta: The American Society of Heating, Refrigerating and Air Conditioning Engineers, 2010.

25. BS2. Airbox system technical manual, http://www.bs2.ch/de/pdf/Download-PDF/Produkte/Airbox100_Datenblatt_De_1-3_31-10-2013.aspx (accessed 21 October 2019).

26. Kim MK and Leibundgut H. Advanced Airbox cooling and dehumidification system connected with a chilled ceiling panel in series adapted to hot and humid climates. *Energ Build* 2014; 85: 72–78.

27. Okamoto S, Kitora H, Yamaguchi H and Oka T. A simplified calculation method for estimating heat flux from ceiling radiant panels. *Energy Build* 2010; 42: 29–33.

28. Hao XL, Zhang GQ, Chen YM, Zou SH and Moschandreas DJ. A combined system of chilled ceiling, displacement ventilation and desiccant dehumidification. *Build Environ* 2007; 42: 3298–3308.

29. Attia S, Lacombe T, Rakotondramiarana HT, Garde F and Roshan G. Analysis tool for bioclimatic design strategies in hot humid climates. *Sustain Cities Soc* 2019; 45: 8–24.

30. Li X, Han Z, Zhao T and Gao J. Online model for indoor temperature control based on building thermal process of air conditioning system. *J Build Eng* 2021; 39: 102270.

31. Deng X and Tan Z. Numerical analysis of local thermal comfort in a plan office under natural ventilation. *Indoor Built Environ* 2020; 29: 972–986.

32. ASHRAE Standard 55-2013. *Thermal environmental conditions for human occupancy*. Atlanta: The American Society of Heating, Refrigerating and Air Conditioning Engineers, 2013.

33. Baldini L, Kim MK and Leibundgut H. Decentralized cooling and dehumidification with a 3 stage LowEx heat exchanger for free reheating. *Energ Build* 2014; 76: 270–277.

34. Kim MK, Leibundgut H and Choi JH. Energy and exergy analyses of advanced decentralized ventilation system compared with centralized cooling and air ventilation systems in the hot and humid climate. *Energy Build* 2014; 79: 212–222.

35. Beausoleil-Morrison I. An algorithm for calculating convection coefficients for internal building surfaces for the case of mixed flow in rooms. *Energy Build* 2001; 33: 351–361.

36. Churchill SW and Usagi R. A general expression for the correlation of rates of transfer and other phenomena. *AIChE J* 1972; 18: 1121–1128.

37. Alamdari F and Hammond GP. Improved data correlations for buoyancy-driven convection in rooms. *Build Serv Eng Res Technol* 1983; 4: 106–112.

38. Awbi HB and Hatton A. Mixed convection from heated room surfaces. *Energy Build* 2000; 32: 153–166.

39. Jeong J-W and Mumma SA. Simplified cooling capacity estimation model for top insulated metal ceiling radiant cooling panels. *Appl Therm Eng* 2004; 24: 2055–2072.

40. Jeong JW and Mumma SA. Practical cooling capacity estimation model for a suspended metal ceiling radiant cooling panel. *Build Environ* 2007; 42: 3176–3185.

41. Kochendoerfer C. Standardized testing of cooling panels and their use in system planning. *ASHRAE Transact* 1996; 102: 651–658.

42. ISO 7730:2005. *Ergonomics of the thermal environment – analytical determination and interpretation of thermal comfort using calculation of the PMV and PPD indices and local thermal comfort criteria.* Geneva: ISO, 2005.

43. Kim MK and Cui S. Evaluation of PMV and PPD Model of a hybrid radiant cooling system. In: *4th international conference on building energy, environment, COBEE2018,* Melbourne, Austrailia, February 5–9 2018; 919–924.

44. ASHRAE. *ASHRAE handbook-fundamental SI edition.* Atlanta: The American Society of Heating, Refrigerating and Air Conditioning Engineers, 2015.

45. Mumma SA. Safety and Comfort Using DOAS Radiant cooling panel systems. *ASHRAE IAQ Appl* 2001; 43(11): 28–32.

46. Kulpmann RW. Thermal comfort and air quality in rooms with cooled ceilings – results of scientific investigations. *ASHRAE Transact* 1993; 99: 448–502.

47. Imanari T, Omori T and Bogaki K. Thermal comfort and energy consumption of the radiant ceiling panel system. Comparison with the conventional all-air system. *Energ Build* 1999; 30: 167–175.

48. Mumma SA. Dedicated Outdoor Air Systems Comfort With DOAS Radiant Cooling System. *ASHRAE IAQ Appl* 2004; 5(4): 22–23.

49. Sastry G and Rumsey P. VAV vs. radiant side-by-side comparison. *ASHRAE J* 2014; 56: 16–24.

50. Niu J and Vanderkooi J. Indoor climate in rooms with cooled ceiling systems. *Build Environ* 1994; 29: 283–290.

51. Mustakallio P, Bolashikov Z, Kostov K, Melikov A and Kosonen R. Thermal environment in simulated offices with convective and radiant cooling systems under cooling (summer) mode of operation. *Build Environ* 2016; 100: 82–91.

52. Schellen L, Loomans MGLC, de Wit MH, Olesen BW and Lichtenbelt WDV. The influence of local effects on thermal sensation under non-uniform environmental conditions – gender differences in thermophysiology, thermal comfort and productivity during convective and radiant cooling. *Physiol Behav* 2012; 107: 252–261.

53. Schellen L, Loomans MGLC, de Wit MH, Olesen BW and Lichtenbelt WDVM. Effects of different cooling principles on thermal sensation and physiological responses. *Energ Build* 2013; 62: 116–125.